PHILOSOPHICAL TRANSACTIONS OF THE ROYAL SOCIETY A MATHEMATICAL, PHYSICAL & ENGINEERING SCIENCES

A Simple Ocean-Atmosphere Coupled Model for the Origin of a Warm El Nino Southern Oscillation Event

T. Yamagata and Y. Masumoto

Phil. Trans. R. Soc. Lond. A 1989 **329**, 225-236
doi: 10.1098/rsta.1989.0072

Phil. Trans. R. Soc. Lond. A **329**, 225–236 (1989)
Printed in Great Britain

A simple ocean–atmosphere coupled model for the origin of a warm El Niño Southern Oscillation event

By T. Yamagata and Y. Masumoto
Research Institute for Applied Mechanics, Kyushu University, Kasuga 816, *Japan*

A simple ocean–atmosphere coupled model is developed to investigate the evolution of a warm El Niño event in the tropical Pacific Ocean. In the absence of climatological winds the model readily evolves a realistic eastward-propagating structure provided that warm sea surface temperature (SST) covers the entire equatorial ocean uniformly. The final state of the model is similar to the mature phase of El Niño. In the presence of realistic climatological winds, however, the model behaves in a different way. It remains in a cold La Niña phase without showing any significant eastward propagation of an air–sea coupled coherent structure. Based on these model results and recent data analyses on the tropospheric quasi-biennial oscillation, it is argued that the Asian summer monsoon before and after the warm phase of El Niño Southern Oscillation is possible.

1. Introduction

It has long been suggested that the Asian summer monsoon has a strong relation with the El Niño Southern Oscillation (ENSO) (Walker & Bliss 1932). Actually, Walker tried to use the Southern Oscillation index as a predictor of devastating Indian summer drought. However, since Bjerknes (1966) suggested that air–sea interaction over the eastern equatorial Pacific is responsible for the rapid evolution of the ENSO phenomena, much attention has been paid to understanding possible mechanisms that give rise to positive feedbacks between the tropical ocean and atmosphere. In particular, the dramatic El Niño of 1982–83 provided a strong stimulus for modelling the major short-term climate variability by use of a variety of ocean–atmosphere coupled models. It is now clear that a positive air–sea feedback plays an important role during the evolution of the warm phase of ENSO (Philander *et al.* 1984; Anderson & McCreary 1985; Zebiak & Cane 1985; Schopf & Suarez 1988). However, we are far from a complete understanding of the basic mechanism of the whole ENSO cycle including triggering and terminating stages. For this purpose we need to clarify what mechanism is most responsible for each ENSO cycle and then to check the mechanism with recent observations. It turns out that we need to shed more light on the suggestion of Walker from a new viewpoint of air–sea–land interaction especially near the western Pacific.

In this paper we first summarize conditions necessary to trigger the warm event. Adopting the precondition in a simplified manner as an initial condition of a simple air–sea coupled model, we show how our simple model captures the overall evolution of both oceanic and atmospheric variables for a canonical warm event. Then we superimpose external winds to demonstrate how the model behaviour is sensitive to ocean mixed-layer physics associated with the winds. On the basis of those model results and observations of the Asian monsoon, we discuss what is most likely to cause and terminate the warm event.

2. Conditions necessary for the warm ENSO events

Recent satellite observations show that the warm sea surface temperature (SST) covered a wide region from the western Pacific to the central Pacific rather quickly before the warm air–sea coupled mode began to evolve in late spring in 1982 or late autumn in 1986 (Nitta 1986; Nitta & Motoki 1987). This quick eastward movement of the SST anomaly as a result of oceanic advection was discussed by Gill (1983) and Harrison & Schopf (1984). The eastward progression of the warm SST is followed by the eastward movement of the active convective system with the intraseasonal periods as discussed by Lau & Chan (1985) and others. A more detailed picture shows that two cross-equatorial cyclonic vortices evolved after strong westerly bursts moved the warm SST further eastward (see Keen 1982).

Figure 1 shows how often those westerly bursts were observed in the western Pacific from 1969 to 1986. The frequency of westerly bursts is abnormally high in the central Pacific in all ENSO years. This is not a surprising result. We notice here that the westerly bursts are well developed in the western Pacific at least in winter and spring before the onset phase of the warm ENSO events.

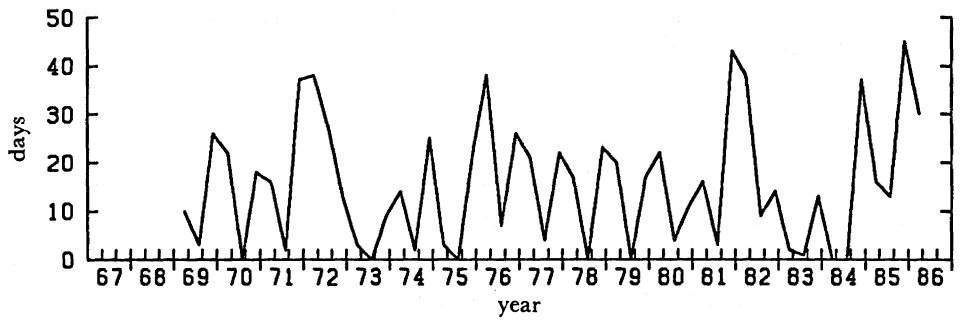

Figure 1. Number of days with westerlies in the western Equatorial Pacific from 1969 to 1986. Adapted from Keen (1987).

On the oceanic side, White *et al.* (1987) showed, using subsurface observation, that a positive anomaly of oceanic heat content (OHC) propagating from the east accumulates in the western Pacific near the Philippine coast in the late autumn and winter one year before that of the mature phase of the ENSO events. Takeuchi (1987) obtained a similar result locked to a seasonal cycle, using a linear shallow water model forced by the Florida State University (FSU) winds. Recently, Miyakoda *et al.* (private communication), using their ocean general circulation model (OGCM) forced by the National Meteorological Center atmospheric data, simulated the 1982–83 event and obtained a similar OHC anomaly pattern in the western equatorial Pacific also in late autumn and winter of 1981. In late spring, this OHC anomaly covers the whole equatorial basin, thus forming the precondition state for the El Niño. It should be noted that this precondition state corresponds to the peak phase of El Niño as defined by Rasmusson & Carpenter (1982). The nomenclature of Rasmusson & Carpenter (1982) is based on the evolution of SST off Peru and is not based on the evolution of Southern Oscillation (SO) indices, which reflect more faithfully the evolution of the air–sea coupled disturbance.

Yasunari (1989) recently found a very high correlation between the western equatorial Pacific SST-OHC anomalies in winter and all India rainfall in summer. Yasunari (1989) also showed that the increase in OHC in the western Pacific is regulated by tropospheric quasi-

biennial oscillations (QBO) locked to a seasonal cycle and is caused by the increase in the Southeast Trade Winds in the autumn, particularly between 140° E and 170° E. The anomalous winds begin with the active Asian summer monsoon, which is also associated with a strong QBO signal (Meehl 1987). The important implication of these new findings is discussed in the final section of this paper.

In short, the above observational and diagnostic results suggest that the mutual cooperation of both atmospheric and oceanic conditions in the western Pacific is necessary to prepare the precondition for the warm phase of ENSO cycles.

3. A COUPLED MODEL

3.1. *Model atmosphere*

The model atmosphere is the spherical version of the Gill's moist model (Yamagata 1987; Davey & Gill 1987). The rudiments are given by Gill (1982). Here we begin with the equations for a primitive, one-mode atmosphere on a sphere. The linearized momentum equations have the form

$$\frac{\partial U}{\partial t} - fV = -\frac{1}{\rho_a a \cos\phi\, \partial\lambda} - \epsilon U, \tag{3.1a}$$

$$\frac{\partial V}{\partial t} + fU = -\frac{1}{\rho_a a\, \partial\phi} - \epsilon V, \tag{3.1b}$$

where (U, V) denote the horizontal velocities at the lower troposphere, p the pressure perturbation, ρ_a air density, f the Coriolis parameter, and a is the radius of the Earth. The variables (λ, ϕ) represent longitude and latitude. The constant ϵ is the coefficient for Rayleigh damping (0.2 per day). Assuming the hydrostatic balance leads to the equation that relates p with the potential temperature perturbation θ. This has the form

$$p = -\rho_a g H_0 \theta/\theta_0, \tag{3.2}$$

where g is the acceleration due to gravity, H_0 is the depth of the lower troposphere and θ_0 is the typical potential temperature. The mass continuity for the lower troposphere takes the form

$$\frac{\partial U}{a\cos\phi\, \partial\lambda} + \frac{\partial V}{a\, \partial\phi} + \frac{W}{H_0} = 0, \tag{3.3}$$

where W is the vertical velocity at the middle level of the troposphere. The potential temperature at the middle level is governed by

$$\frac{\partial \theta}{\partial t} + \frac{\theta_0 N^2}{g} W = Q - \gamma_a \theta \tag{3.4}$$

where N is the buoyancy frequency, γ_a is the coefficient of newtonian cooling (0.2 per day) and Q is the heating rate. This Q is related to the precipitation rate P in the following way

$$Q = \rho_w L_c P/(\rho_a H_0 C_p), \tag{3.5}$$

where ρ_w is the water density, L_c is the latent heat of condensation and C_p is the specific heat of air at constant pressure. The precipitation rate P is predicted by the linearized equation that governs the moisture per unit area

$$\bar{q}\left(\frac{\partial U}{a\cos\phi\, \partial\lambda} + \frac{\partial V}{a\, \partial\phi}\right) = E - P, \tag{3.6a}$$

PHILOSOPHICAL TRANSACTIONS OF THE ROYAL SOCIETY A MATHEMATICAL, PHYSICAL & ENGINEERING SCIENCES

for $q = \bar{q}$ and $P > 0$, and

$$\frac{\partial q}{\partial t} + \bar{q}\left(\frac{\partial U}{a\cos\phi\,\partial\lambda} + \frac{\partial V}{a\partial\phi}\right) = E, \tag{3.6b}$$

for $q < \bar{q}$ or $q = \bar{q}$ and $P \leqslant 0$, where $\bar{q}$ is the moisture per unit area for which the atmosphere is just saturated. We assume that $\bar{q}$ is always given by the saturated value (6.3 cm) at 26 °C. The perturbation evaporation E is given by

$$E = -\delta(\bar{q} - \bar{q}_s(T_s)), \tag{3.7}$$

where δ is 0.14 per day and $\bar{q}_s$ is the saturated moisture at the sea surface temperature T_s. Linearizing the Clapeyron–Clausius relation around the saturated moisture $\bar{q}$ at 26 °C, we obtain

$$\bar{q}_s(T_s) = \bar{q}(1 + 0.059(T_s - 26)). \tag{3.8}$$

Now it is convenient to introduce a new quantity H defined by

$$H = \frac{H_0\theta}{\theta_0}\left(= -\frac{p}{\rho_a g}\right). \tag{3.9}$$

Then the potential temperature equation (3.4) is replaced by

$$\frac{\partial H}{\partial t} - H_e\left(\frac{\partial U}{a\cos\phi\,\partial\lambda} + \frac{\partial V}{a\,\partial\phi}\right) = -\gamma_a H, \tag{3.10a}$$

for $q < \bar{q}$ or $q = \bar{q}$ and $P \leqslant 0$, and

$$\frac{\partial H}{\partial t} - (H_e - H_m)\left(\frac{\partial U}{a\cos\phi\,\partial\lambda} + \frac{\partial V}{a\,\partial\phi}\right) = \frac{H_m}{\bar{q}} - \gamma_a H, \tag{3.10b}$$

for $q = \bar{q}$ and $P > 0$, where the equivalent depth $H_e (= N^2 H_0^2/g)$ and the negative contribution due to moist processes $H_m (= \rho_w L_c \bar{q}/(\rho_a \theta_0 C_p))$ are used for simplicity. We assume $H_e =$ 450 m and $H_m = 395$ m for a coupled model. Thus the phase speed of a moist Kelvin wave is 23 m s^{-1}.

3.2. *Model ocean*

The model ocean is the spherical version of the Anderson–McCreary model. The reason we adopt the model is that it is the simplest model that includes the ocean thermodynamics explicitly. The details are described in the original paper (Anderson & McCreary 1985). Here we only refer to the equations. Those are

$$\frac{\partial(h\boldsymbol{u})}{\partial t} + \boldsymbol{u}\cdot\nabla(h\boldsymbol{u}) + h\boldsymbol{u}\nabla\cdot\boldsymbol{u} - f\boldsymbol{k}\times(h\boldsymbol{u}) = -\nabla(\tfrac{1}{2}\alpha g T h^2) + \nu_h\nabla^2(h\boldsymbol{u}) + \boldsymbol{\tau}, \tag{3.11a}$$

$$\frac{\partial h}{\partial t} + \nabla\cdot(h\boldsymbol{u}) = \frac{2\delta_0}{h^2 T} - w + \gamma_0\left(\frac{T - T^*}{T}\right), \tag{3.11b}$$

$$\frac{\partial T}{\partial t} + \boldsymbol{u}\cdot\nabla T = \frac{2}{h}\left(-\gamma_0(T - T^*) - \frac{\delta_0}{h_2}\right) + \nu_h\nabla^2 T, \tag{3.11c}$$

where T is the mixed layer temperature minus that of the deep layer (19.5 °C in the present model), $\boldsymbol{\tau}$ is the wind stress proportional to the wind and other quantities are defined in the usual way. The values of lateral eddy viscosity ν_h, thermal expansion coefficient α, upwelling velocity from the deep layer w, entrainment coefficient δ_0, thermal relaxation coefficient γ_0 are

1×10^8 cm^2 s^{-1}, 3×10^{-4} K^{-1}, 2.67×10^{-5} cm s^{-1}, 6×10^4 cm^3 K s^{-1} and 2×10^{-4} cm s^{-1}, respectively. T^* exactly follows the expression of Anderson & McCreary (1985):

$$T^* = 4 + \tfrac{1}{2}(11.33 - 4)\,(1 + \cos 2\pi y / y_N), \tag{3.12}$$

where $y_N = 90°$ in the present model. The model ocean covers the area from 50° S to 50° N, 140° E to 80° W. The steady solution without motion for the above set of thermal parameters has $T = 10°$ C and $h = 150$ m at the Equator.

4. Model results

4.1. *Case I. A bounded ocean without external wind forcing*

As we have summarized in §2, the warm SST and positive oceanic heat content anomaly cover almost all of the equatorial Pacific at the precondition stage for the air–sea coupled disturbance. This state is established rather quickly by the oceanic processes. Here we demonstrate how the air–sea coupled disturbance evolves under this non-equilibrium state by use of the coupled model described in §3.

As for the precondition state of the model, we assume that the equatorial oceanic mixed-layer temperature is 29° C. Because the atmosphere is assumed to be saturated by moisture at 26° C, convective heating occurs wherever low-level winds converge.

Figure 2 shows the time evolution of zonal winds, currents and mixed-layer depth anomalies along the Equator. For the first 150 days the maximum westerly wind stays near the western boundary of the model Pacific. Then it begins to move eastward with a phase speed of about 0.5 m s^{-1}. After one year it reaches the eastern Pacific and stays there. The area of active precipitation also shifts toward the eastern Pacific with a phase speed of about 0.5 m s^{-1}. A sharp front of a positive mixed-layer depth anomaly is generated during the initial stage and propagates as the oceanic Kelvin wave with a phase speed of about 2 m s^{-1}. In the wake of this front, a positive zonal gradient of the mixed layer depth associated with eastward currents is sustained by the eastward moving westerly wind anomaly. This whole air–sea coupled system propagates eastward slowly with a phase speed of about 0.5 m s^{-1} and settles down into a mature phase of the ENSO.

The overall model evolution pattern is quite similar to those of the 1982–83 and 1986–87 events. This also suggests that the preconditioning was completed by the late spring in 1982 and by the late autumn in 1986. The above results demonstrate that the air–sea coupled disturbance can actually evolve from the prescribed non-equilibrium state. This is consistent with the important finding of Zebiak & Cane (1987) that equatorial heat content increases before model warm events.

The time section of the oceanic zonal velocity along the equator shows that the Kelvin wave excited during the initial adjustment process reflects as the Rossby waves at the eastern boundary (figure 2). However, the reflected waves decay rather quickly because the atmospheric winds and oceanic currents are negatively correlated (Yamagata 1985).

The present experiment corresponds to Model IV of Hirst (1988). Therefore one might expect that the evolution of the coupled disturbance should be described by the U1 mode of Hirst (1988). We must note, however, that the present coupled disturbance has a finite amplitude. Even if the disturbance is very weak initially so that it can be predicted well by the linear theory as shown by Hirst (1988), it grows eventually into a finite amplitude. The

PHILOSOPHICAL TRANSACTIONS OF THE ROYAL SOCIETY A MATHEMATICAL, PHYSICAL & ENGINEERING SCIENCES

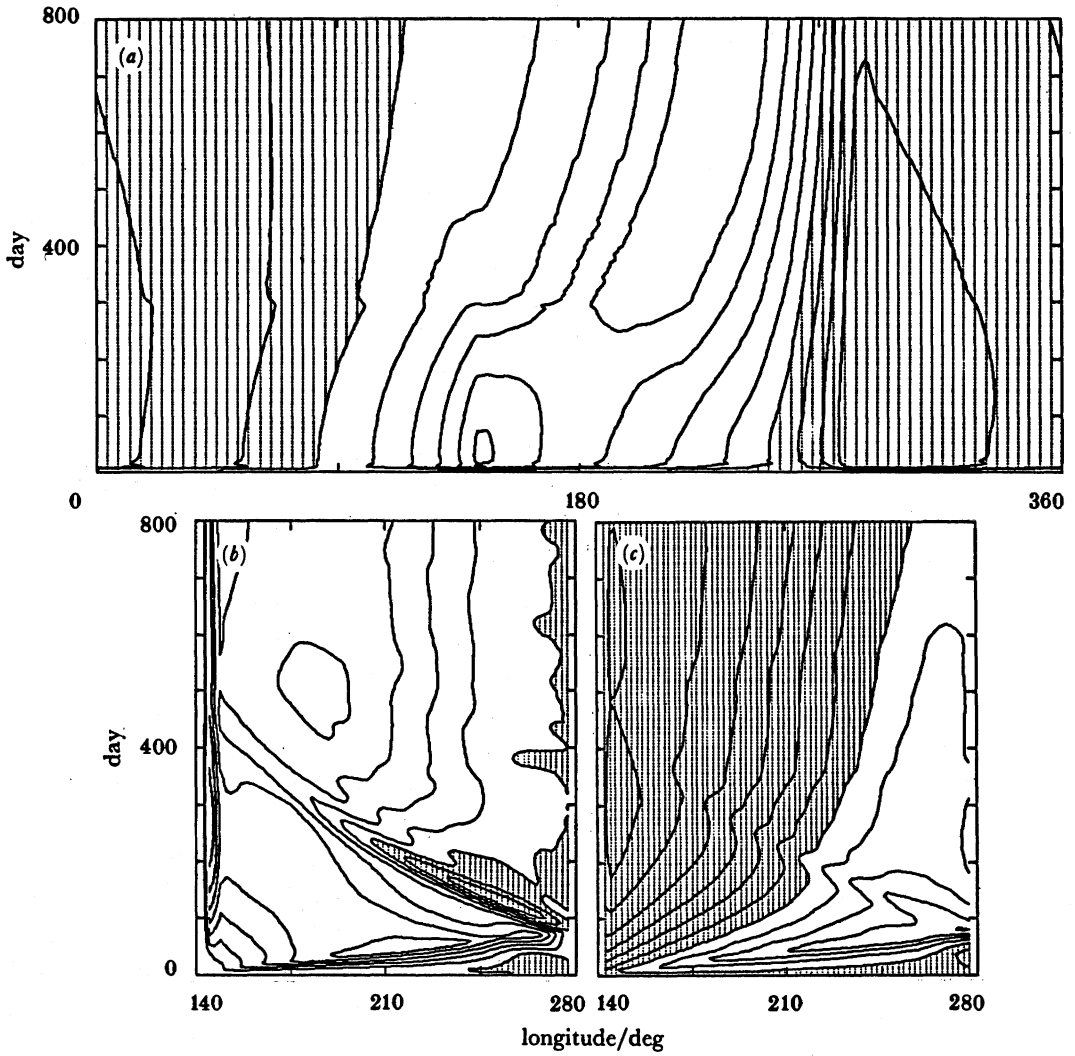

FIGURE 2. Time evolution of (*a*) zonal winds, (*b*) zonal currents and (*c*) mixed-layer depth anomalies along the Equator for Case I. The contour intervals are 1 m s^{-1}, 0.1 m s^{-1} and 10 m, respectively. Areas of easterly winds, easterly currents and negative depth anomalies are shaded.

westerly wind associated with this finite amplitude disturbance changes the basic oceanic mixed layer structures so that the Rossby waves excited at the eastern boundary are even more damped. This is why the results of Hirst (1988) are of limited applicability.

4.2. *Case II. An unbounded ocean model*

It is of interest to see what happens in the case of a planet covered by water. It turns out that the present case is useful for understanding how the coupled structure is triggered by atmospheric disturbances. We assume that the ocean temperature is 29 °C all over the tropics as in §4.1 so that the convective heating occurs wherever low-level winds converge. If there is no inhomogeneity in the zonal direction, the coupled system is calm in the tropics, whereas geostrophic winds blowing eastward are excited in off-equatorial regions. To generate the air–sea coupled coherent structure we perturb the ocean by applying equatorial westerly wind bursts, with a zonal extent of 60°, for about 10 days. Figure 3 shows the time evolution of

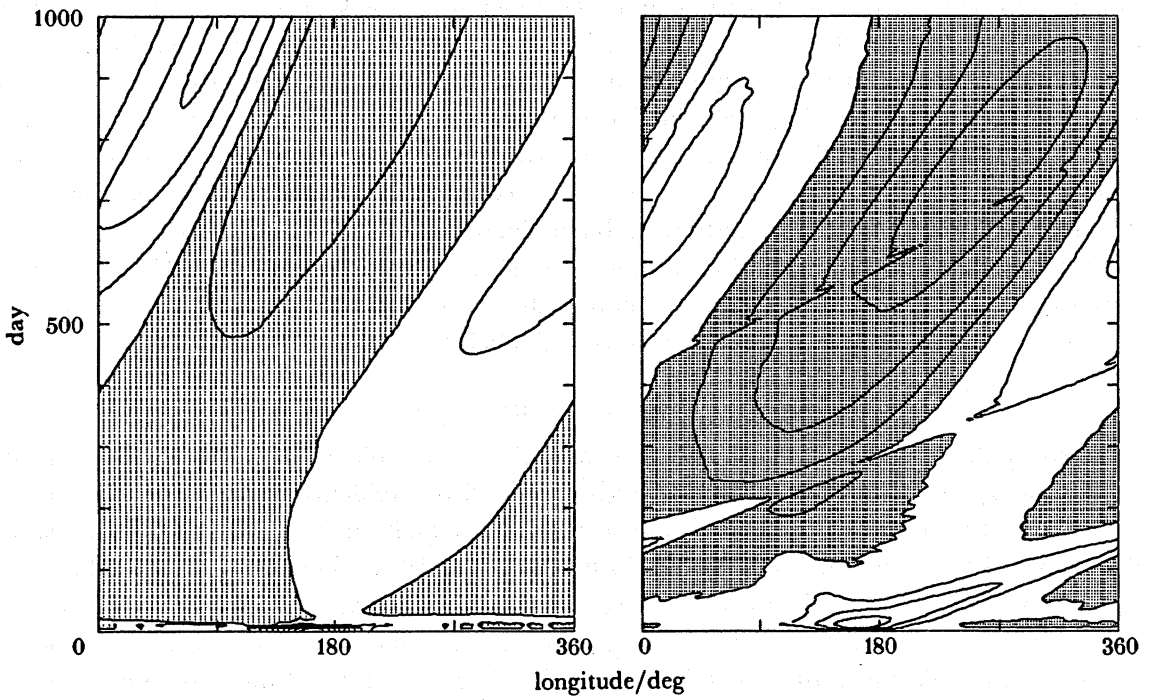

FIGURE 3. Time evolution of (*a*) zonal winds and (*b*) zonal currents along the equator for Case II (initial westerly bursts of which maximum speed is 10 m). The contour intervals are 1 m s^{-1} and 0.1 m s^{-1}, respectively. Areas of easterly winds and easterly currents are shaded.

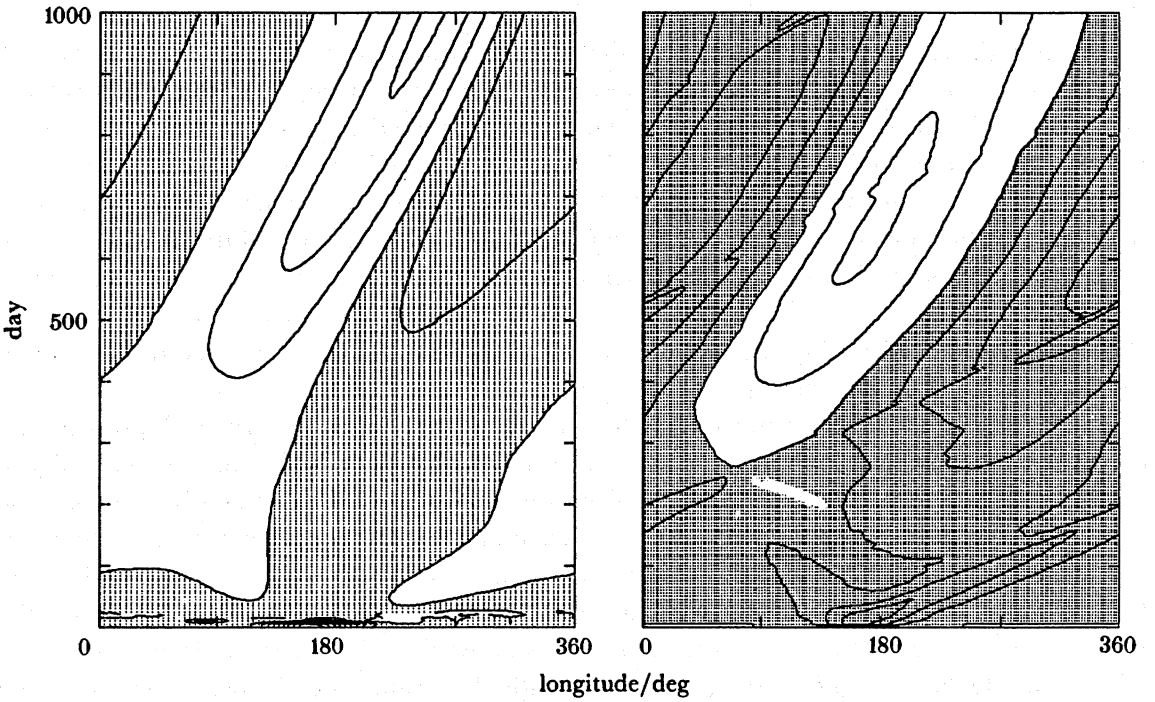

FIGURE 4. As in figure 3 but for the initial easterly bursts.

atmospheric zonal winds and oceanic zonal currents after this kick along the Equator. It is clearly demonstrated that three kinds of disturbances evolve in the coupled system: atmospheric, oceanic (free and forced) and ocean–atmosphere coupled disturbances. The Kelvin waves generated by the winds cause weak but long-lasting ocean temperature anomalies, which trigger the air–sea coupled distrubance. The case in which there are easterly wind bursts shows a little different behaviour: a coupled disturbance cannot be generated directly by the kick as in the westerly wind bursts (figure 4). This is because the easterly bursts cannot generate that synthesis of an atmospheric forced Rossby response (the Matsuno–Gill pattern) and an oceanic warm-water anomaly with positive zonal gradient, which is favourable for the air–sea coupled coherent structure (see Yamagata 1987).

4.3. *Case III. A bounded ocean with external wind forcing*

To study the effect of external winds that mimic the climatological winds, two experiments were done by using the climatological winds described by Goldenberg & O'Brien (1981).

In the first experiment, the magnitude of the winds is maintained. This run does not show the eastward movement of the coupled disturbance and settles down into the cold La Niña phase. This may be caused by the existence of the upwelled cold area in the central and eastern Pacific. In the second experiment, the magnitude of the winds is reduced to one half of the original values. This measure was taken to simulate the weakening of the annual cycle in the tropical Indian and Pacific sectors (cf. Meehl 1987). The result of this second run is quite similar to the case without external wind forcing: the coupled disturbance generated in the western Pacific propagates eastward into the eastern part of the Pacific. The upwelling associated with the external winds is so weak that it cannot stop the eastward intrusion of the disturbance.

To check the results of this section we coded a model equivalent to the Anderson–McCreary model except for (*a*) a time-dependent atmosphere, (*b*) values of δ_0, γ_0 and w four times as large as the original values and (*c*) heating over land is proportional to positive SST anomaly in the western equatorial Pacific. The measure (*b*) was taken to reduce the period of model ENSO cycles. Three experiments were done with this model. The first run without external heating over land in the west showed the recurrent generation of air–sea coupled disturbances in the western Pacific at first but finally the model settled down into El Niño state as expected from the result of §4.1 (figure 5). This damped oscillation involves the reflection of oceanic warm Rossby waves excited during the initial adjustment because it takes about 300 days for them to travel across the whole ocean basin.

The second run with heating over land in the west showed an eastward propagating oscillatory mode as in Anderson & McCreary (1985) with a period of about 500 days (figure 6). This oscillatory mode was excited also from the final state of the first run by applying the heat source over land. Before one warm event is over, another warm event occurs gradually in the western Pacific and propagates into the eastern Pacific. This may be interpreted in the following way. When one warm event reaches its maximum near the eastern boundary, the westerly wind associated with the disturbance becomes weak in the central and western Pacific. This is simply because the heating associated with the disturbance is located far from the western boundary. Then there is room for the easterly winds associated with the heating over land in the west to prevail in the western and central equatorial Pacific. This is especially true in the Anderson–McCreary model in which atmospheric damping rate is assumed to be rather

PHILOSOPHICAL TRANSACTIONS OF THE ROYAL SOCIETY A MATHEMATICAL, PHYSICAL & ENGINEERING SCIENCES

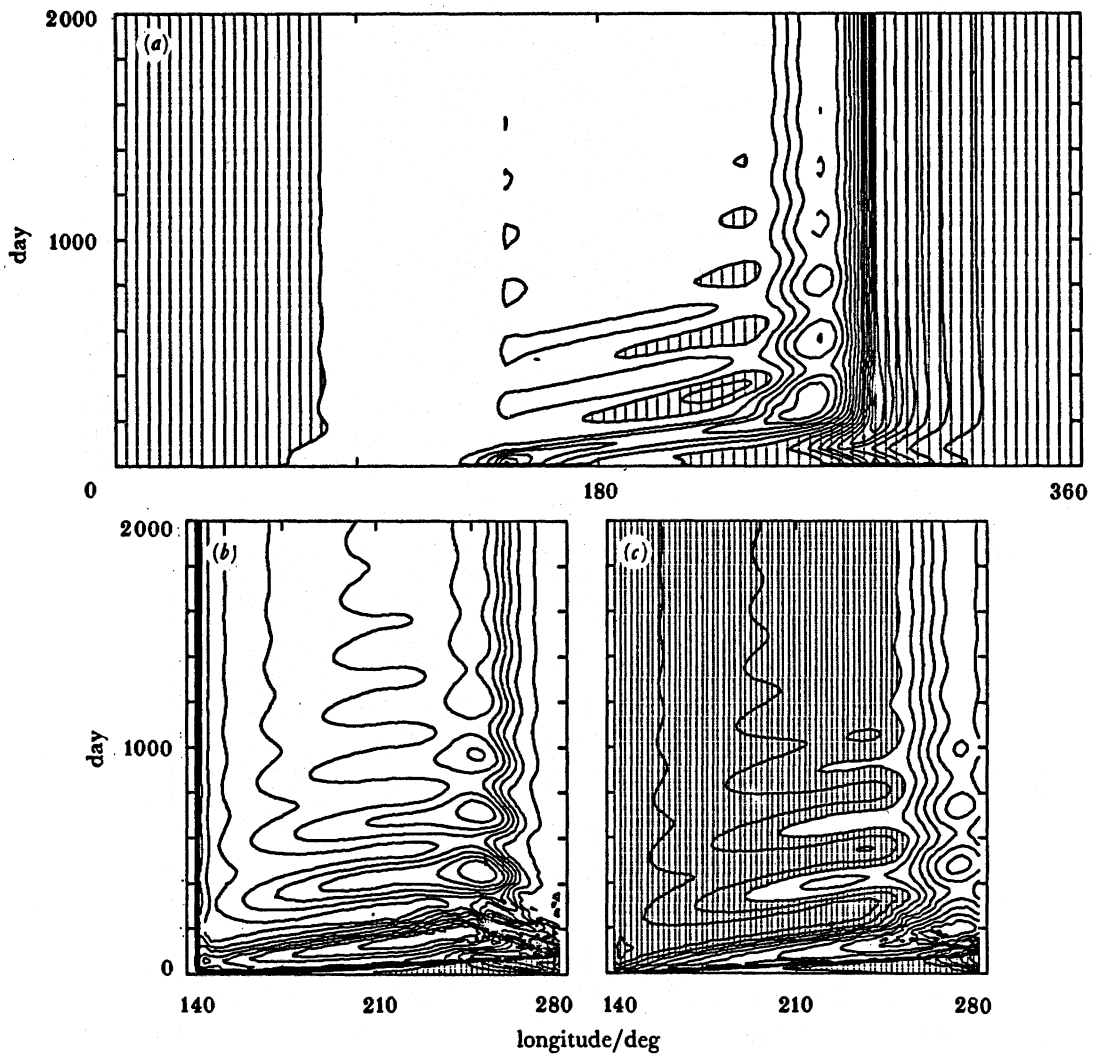

FIGURE 5. Time evolution of (*a*) zonal winds, (*b*) zonal currents and (*c*) mixed-layer depth anomalies along the Equator for the Anderson–McCreary model without heating over land. The contour intervals are 2 m s^{-1}, 1 m s^{-1} and 10 m, respectively. Areas of easterly winds, easterly currents and negative depth anomaly are shaded.

big (about 2.6 per day). The equatorial upwelling associated with the easterly winds not only kill the warm event but also cancel the cold state in the western Pacific by piling up warm water near the boundary. The westerly winds associated with this increased heating convey the warm water to the equatorial area and excite another warm coupled disturbance in the western Pacific (see §4.2).

The above scenario for the origin of the warm ENSO event is very different from other model studies such as Zebiak & Cane (1987), Schopf & Suarez (1988) and Battisti (1988), in which the western boundary reflection of Rossby waves excited in the eastern Pacific during a cold event plays a crucial role in triggering the next warm event. The third run, in which heating is three times stronger than in the second run, settled down into a cold La Niña state. This is because the equatorial upwelling excited by the easterly winds is too strong for a warm air–sea coupled disturbance to propagate eastward.

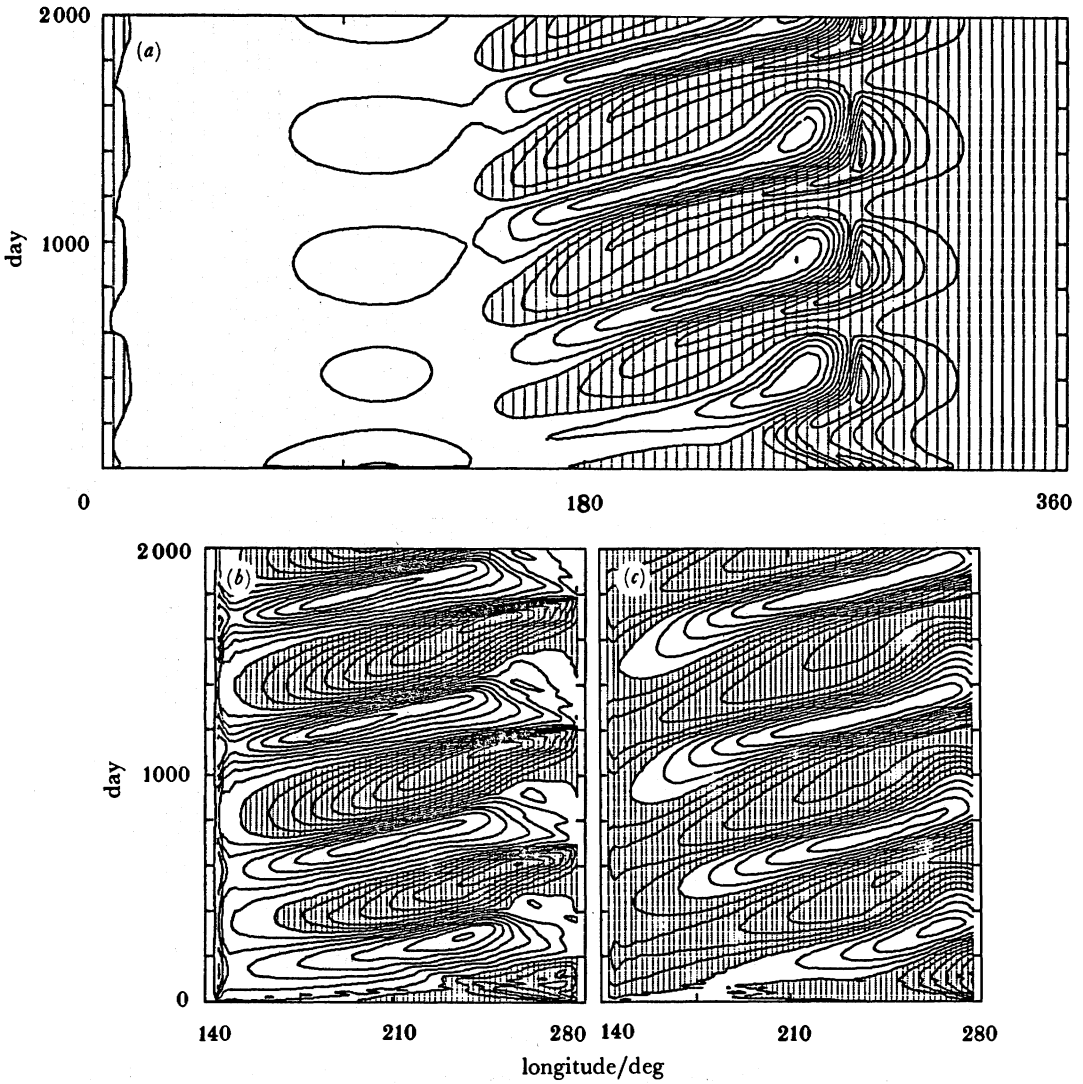

FIGURE 6. As in figure 5 but for the case with heating over land. The heating is parametrized according to the expression of latent heat release (equation (3.5) of Anderson & McCreary (1985)) by use of the temperature at the western edge of the ocean. The value of an amplitude factor is 0.075 $m^2 s^{-3}$.

5. DISCUSSION

We have shown, by use of a simple coupled model, that a warm ENSO mode similar to observations evolves automatically provided that warm SST and OHC anomalies cover the equatorial Pacific. We have suggested that both atmospheric westerly bursts and oceanic anomalous OHC in the western Pacific are necessary for this preconditioning. As mentioned in §1, Yasunari (1989) found a high positive (negative) correlation (*ca.* ± 0.8) between the warm (cold) SST–OHC anomaly in the western equatorial Pacific in the winter before the mature ENSO year, and rainfall over India during the preceding (following) summer. This suggests that the strong quasi-biennial oscillation of the Asian summer monsoon plays a key role in ENSO cycles (Meehl 1987). In particular, the active (inactive) summer monsoon is followed by increasing anomalous easterly (westerly) winds in the western Pacific (figure 7). This suggests that a positive feedback mechanism exists in the air–sea–land system.

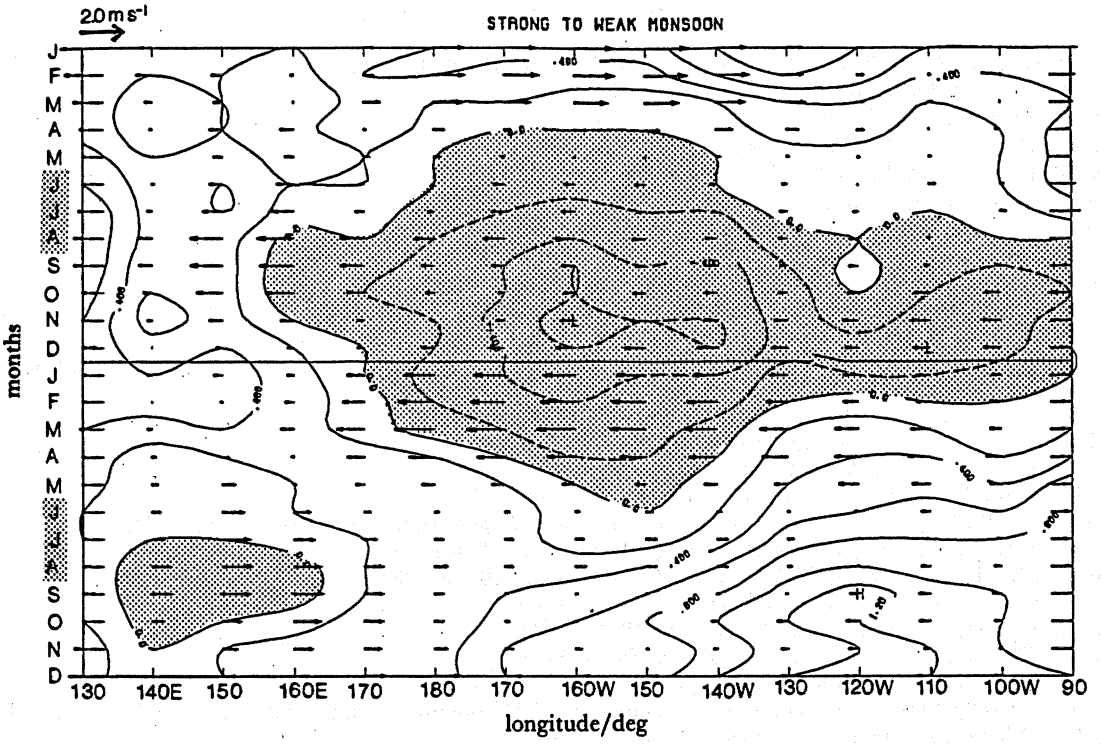

FIGURE 7. Longitude–time section of anomalous SST and zonal winds at 700 mbar† along the Equator. Composite for two years from a strong Indian summer monsoon to a weak Indian summer monsoon. Negative SST anomaly is shaded. From Yasunari (1989).

Recently, Parthasarathy *et al.* (1987) have reported a high positive correlation (greater than 0.8) between 850 mbar anomalous westerlies during the mature phase of the ENSO events and rainfall over India during the following summer. This is also seen in figure 7 and suggests that the Asian summer monsoon revives very strongly after the mature phase of the warm ENSO events and thus terminates them. The QBO aspect of ENSO appears to be a firm indication that the birth and death of ENSO is regulated by the Asian summer monsoon followed by the air–sea–land interaction in the western Pacific.

The results presented here, and those of Anderson & McCreary (1985), both of which take the external wind forcing into account explicitly, are consistent with this picture and suggest that the origin of the warm ENSO event is a result of warm water accumulated near the Equator by the anomalous westerly winds. The termination of ENSO may be explained by anomalous easterly winds that blow towards the warm water accumulated in the western Pacific.

It seems clear that at least two important problems are left to be solved for an understanding of ENSO cycles. Firstly we must explain why the Asian summer monsoon revives so strongly and thus terminates so rapidly the mature phase of the warm ENSO events. Secondly, we must explain why the westerly bursts occur so frequently only in the wintertime one year before the mature phase of the warm ENSO events. The latter is directly related to the predictability of the origin of the warm air–sea coupled mode. A model that simulates ENSO cycles in a realistic way will have an air–sea–land process possibly including Eurasian and Himalayan snow cover as a minimum prerequisite (see Blandford 1884).

† 1 mbar = 10^2 Pa.

PHILOSOPHICAL TRANSACTIONS OF THE ROYAL SOCIETY A MATHEMATICAL, PHYSICAL & ENGINEERING SCIENCES

References

Anderson, D. L. T. & McCreary, J. P. 1985 *J. atmos. Sci.* **42**, 615–628.
Battisti, D. S. 1988 Ph.D. thesis, University of Washington.
Bjerknes, J. 1966 *Tellus* **18**, 820–829.
Blandford, H. F. 1884 *Proc. R. Soc. Lond.* A **37**, 3–22.
Davey, M. K. & Gill, A. E. 1987 *Q. Jl R. met. Soc.* **113**, 1237–1269.
Gill, A. E. 1982 *Geophys. Astrophys. Fluid Dynam.* **19**, 119–152.
Gill, A. E. 1983 *J. phys. Oceanogr.* **13**, 586–606.
Goldenberg, S. O. & O'Brien, J. J. 1981 *Mon. Wea. Rev.* **109**, 1190–1207.
Harrison, D. E. & Schopf, P. S. 1984 *Mon. Wea. Rev.* **112**, 923–933.
Hirst, A. C. 1988 *J. atmos. Sci.* **45**, 830–852.
Keen, R. A. 1982 *Mon. Wea. Rev.* **110**, 1405–1416.
Keen, R. A. 1987 In *Proceedings of the U.S. TOGA Western Pacific Air–Sea Interaction Workshop* (ed. R. Lukas & P. Webster). UCAR.
Lau, K. M. & Chan, P. H. 1985 *Mon. Wea. Rev.* **113**, 1889–1901.
Meehl, G. A. 1987 *Mon. Wea. Rev.* **115**, 27–50.
Nitta, T. 1986 *J. met. Soc. Japan.* **64**, 373–390.
Nitta, T. & Motoki, T. 1987 *J. met. Soc. Japan.* **65**, 497–506.
Parthasarathy, B., Poly, G. W. & Weickmann, K. M. 1987 *Tropical Ocean–Atmosphere Newsletter.* **41**, 3–7.
Philander, S. G. H., Yamagata, T. & Pacanowski, R. C. 1984 *J. atmos. Sci.* **41**, 604–613.
Rasmusson, E. M. & Carpenter, T. H. 1982 *Mon. Wea. Rev.* **110**, 354–384.
Schopf, P. S. & Suarez, M. J. 1988 *J. atmos Sci.* **45**, 549–566.
Takeuchi, K. 1987 *Geophys. Bull. Hokkaido Univ.* **49**, 381–386.
Walker, G. T. & Bliss, E. W. 1932 *Mem. R. met. Soc.* **4**, 53–84.
White, W. B., Pazan, S. E. & Inoue, M. 1987 *J. phys. Oceanogr.* **17**, 264–280.
Yamagata, T. 1985 Stability of a simple air–sea coupled model in the tropics. In *Coupled ocean–atmosphere models* (ed. J. C. J. Nihoul). Amsterdam: Elsevier.
Yamagata, T. 1987 *J. met. Soc. Japan* **65**, 153–165.
Yasunari, T. 1989 *J. Climat.* (In the press.)
Zebiak, S. E. & Cane, M. A. 1987 *Mon. Wea. Rev.* **115**, 2262–2278.

PHILOSOPHICAL TRANSACTIONS OF THE ROYAL SOCIETY A MATHEMATICAL, PHYSICAL & ENGINEERING SCIENCES